The Effect of Imidazolium-based Ionic Liquid on Oxidation Kinetics of Coal

Deng J.[1,2], Bai Z.J.[1,*], Wang C.P.[1,2], Luo Z.M.[1,2], Wang Y.C.[1,2]

[1] *School of Safety Science and Engineering, Xi'an University of Science and Technology, Xi'an, Shaanxi, China*
[2] *Shaanxi Key Laboratory of Prevention and Control of Coal Fire, Xi'an University of Science and Technology, Xi'an, Shaanxi, China*
**Corresponding author's email: 1693058198@qq.com*

ABSTRACT

To investigate the effects of ionic liquids (ILs) on the oxidative combustion characteristics of coal, four types of imidazole ([EMIm][BF_4], [BMIm][BF_4], [BMIm][NO_3], [BMIm][I]) were selected to treat coal samples; pr-[BMIm][BF_4] was processed one month ago. The thermogravimetry (TG) experiments and oxidation kinetics analysis methods were employed to study the oxidation characteristics of ILs on coal, such as characteristic temperature, thermal mass loss rate, and oxidation kinetics characteristic parameters. The results showed that the characteristic temperatures of the treated coal samples increased. Among them, the [BMIm][I]-treated coal samples increased cracking temperature (T_1), maximum oxidization mass gain (T_2), ignition temperature (T_3), burnout temperature (T_4), minimum thermal rate (T_a), maximum thermal energy (T_b), and maximum thermal rate (T_c) by 33.2, 29.3, 20.7, 42.8, 11.4, 23.0, and 27.9°C, respectively. The increase mass ratio of coal samples treated with ILs increased and decreased at the water evaporation and thermal decomposition stages. The apparent activation energy (E_a) of coal samples treated with ILs increased, and the mechanism function also changed accordingly. These showed that the ILs improved the thermal stability of the coal samples in the stages of absorbing oxygen and increased mass, and the loss of combustion. The ILs caused damage to the molecular structure of the coal, and ultimately effected changes in the combustion performance. In addition, the combustion properties of the coal sample treated before one month were the same, indicating that the [BMIm][BF_4] did not weaken the inhibitory effectiveness of the coal sample over time, coal spontaneous combustion could be effectively suppressed.

KEYWORDS: Oxidation, thermal stability, inhibition

NOMENCLATURE

A	pre-exponential factor (1/min)
E_a	apparent activation energy (J/mol)
R	universal gas constant 8.3143 J/(K·mol)
T_1	cracking temperature (°C)
T_2	maximum oxidization mass gain (°C)
T_3	ignition temperature (°C)
T_4	burnout temperature (°C)
T_a	temperature of minimum thermal rate (°C)
T_b	temperature of maximum thermal energy (°C)
T_c	temperature of maximum thermal rate (°C)
r	correlation coefficient

Greek

α	conversion
β	heating rate (°C/min)

INTRODUCTION

Coal resources are mainly bituminous coal and lignite, and more than 90% of coal seams have a

Proceedings of the Ninth International Seminar on Fire and Explosion Hazards (ISFEH9), pp. 1154-1163
Edited by Snegirev A., Liu N.A., Tamanini F., Bradley D., Molkov V., and Chaumeix N.
Published by Saint-Petersburg Polytechnic University Press
ISBN: 978-5-7422-6498-9 DOI: 10.18720/spbpu/2/k19-12

tendency for spontaneous combustion in classes I and II. Coal spontaneous combustion is extremely serious, not only causing major property damage, but also resulting in significant personal injury and death [1, 2]. Therefore, the inhibition of coal spontaneous combustion has become the main direction for mine fire prevention.

To scientifically, effectively, and fundamentally inhibit coal spontaneous combustion, numerous mine fire inhibition technologies have been developed which include resistance, inerting, and cooling [3, 4]. Among them, physical inhibitors are the most popular, altering physical effects of the coal body and the surrounding environment. As time goes on, the inhibiting capacity gradually declines until it disappears completely [5–8]. Therefore, the development of chemical inhibitors can effectively destroy coal microscopic active groups and inhibit the active structure on the surface of coal molecules to forestall coal spontaneous combustion [9, 10]. The current research showed that in coal spontaneous combustion the functional groups in the coal molecules react with oxygen continuously to release heat and accumulate, which, in turn, causes the coal body to heat [11, 12]. ILs are environmentally friendly green solvents with low volatilization, low distillation, odorless, non-combustible, easy to handle, and have high applicability [13]. The results showed that different ILs could reduce the oxidation characteristics and dissolve and destroy the microscopic active structure on the surface of coal molecules, which could fundamentally destroy the microscopic active groups of coal or inhibit the active structure of coal to prevent spontaneous combustion [14]. Studies of liquefaction, extraction, and desulfurization consistently concluded that ILs could break hydrogen bonds, covalent bonds, and carbonyl groups in the side chains of coal molecules. Due to the electrical covalent bond balance of the coal molecule, it was destroyed by the π bond contained in the anion and cation in ILs [15–23]. In the oxidative heating process of treating coal with ILs, studies have pointed out that ILs could reduce the oxidation characteristics of coal, of the released index gases, and of the mass loss rate [24–27]. Above studies were summarized to show that the inhibiting of coal by ILs mainly destroyed and dissolved the active groups of coal, including hydrogen bonds, aromatic structures, aliphatic chain hydrocarbons, and oxygenates, such as hydrocarbon groups, carbonyl groups, and ether bonds, methyl, methylene aliphatic side chain group. The aromatic ring structure of coal molecules was relatively stable and could not be destroyed. The main reason for hindering the oxidation process of coal is that the oxygen-removing ability of coal molecules is weakened. The formation of stable carbonyl groups is increased, and the quantity of active carbonyl groups is reduced. The low-temperature oxidation activity of coal is closely related to hydrogen bonding, and the reduction of hydrogen bonding causes the oxidation activity of coal to be weakened to varying degrees.

In this paper, the oxidation kinetics method was used to study the kinetic characteristics of coal samples treated with ILs in the process of spontaneous combustion, such as characteristic temperature, E_a, and $\ln A$. To investigate that the inhibiting effect does not decrease with time, the inhibition ability of the coal sample treated before one month was studied. This paper provides an in-depth understanding of the spontaneous combustion process of coal oxidation and provides scientific and effective indicators and theoretical basis for the oxidative coal spontaneous combustion in different inhibitory stages. Therefore, it opens up new scientific and technological techniques for inhibiting coal spontaneous combustion.

EXPERIMENTAL

Materials

Coal sample preparation

The fresh lignite sample used in this study was obtained from Wangwa, Ningxia, China. It was ground and pulverized to a size of approximately 200–280 μm. The coal sample was vacuum dried

at room temperature for 24 h, sealed and stored in the dark, Table 1 lists the coal quality indicators.

Table 1. Coal quality indicators of the coal samples

Sample	M_{ad}/%	A_{ad}/%	V_{ad}/%	FC_{ad}/%	H/%	C/%	N/%	S/%
lignite	10.31	9.71	35.54	44.44	3.391	64.15	1.338	1.641

IL preparation

Four ILs, considering the sound dissolution and destruction properties, namely 1-ethyl-3-methylimidazolium tetrafluoroborate ([EMIm][BF_4]), 1-butyl-3-methylimidazolium iodide ([BMIm]I), 1-butyl-3-methylimidazolium tetrafluoroborate ([BMIm][BF_4]), 1-butyl-3-methylimidazolium nitrate ([BMIm][NO_3]), were from the Lanzhou Institute of Physical Chemistry of the Chinese Academy of Sciences, with a purity of over 99 mass% [28].

IL treatment of coal subsamples

The coal sample and the four ILs were thoroughly mixed in a ratio of 1:2 (g:mL), and stirred eight hours. Taking into account the interference of the IL on the experimental process, the mixture was rinsed by a centrifuge, and the distilled water was repeatedly washed. By measuring the pH of the solution, until the acidity and alkalinity of the coal samples no longer changed. The rinse was placed in a specific bottle for recycling to avoid contamination of the environment. Then, it was vacuum dried at 27 °C for 48 hours until the mass did not change, and the treated sample was obtained, which was sealed and stored. To study whether the IL inhibit to coal samples would degrade over time, [BMIm][BF_4] treated coal samples were produced before 30 days and termed Pr-[BMIm][BF_4]. To avoid the influence of distilled water on the error of the results, the same process was used to prepare distilled water to wash the coal sample as a comparative coal sample. The coal samples treated with [EMIm][BF_4], [BMIm][BF_4], [BMIm][NO_3], [BMIm][I], Pr-[BMIm][BF_4] and H_2O were defined as EBTC, BBTC, BNTC, BITC, PBBTC, and HTC, respectively.

Experimental procedure

Six coal samples were conducted by the German NETZSCH STA409PC DSC-TGA synchronous thermal analyzer. The procedure was strictly followed by an operating procedure with a mass of ca. 10.0 mg per sample. The sample was heated in an air atmosphere at a temperature ranging from 30.0 to 800.0 °C at a heating rate of 10 °C/min.

RESULTS AND DISCUSSION

Characteristics of coal oxidation pyrolysis curve

Characteristic temperature

Figure 1 shows the pyrolysis curve of the EBTC sample during oxidation. Experiments showed that the trend of TG-DTG curves for treating coal samples was different. It is generally considered that T_1 is the maximum evaporation of water and desorption of gases and called “dry cracking temperature”; T_2 represents the maximum oxidization mass gain. T_3 is the ignition point; T_4 is the temperature burnout point corresponding to the complete combustion. Therefore, the entire process of oxidizing coal from oxygen to combustion is divided into five stages. Stage Ⅰ is called the water evaporation mass loss stage (starting temperature T_0–T_1; oxygen absorption mass increase stage (T_1–T_2) is stage Ⅱ; coal thermal decomposition stage (T_2–T_3) is classified into stage Ⅲ; stages Ⅳ and Ⅴ are the combustion stage (T_3–T_4) and the complete burnout stage (T>T_4), respectively. TG and DTG curves of the BBTC, BNTC, BITC, PBBTC, and HTC subsamples are illustrated in

Fig. 2. Figure 3 describes the DSC and DDSC curves for the BBTC, BNTC, BITC, PBBTC, and HTC subsamples. Considering that oxygen absorption mass increase stage and thermal decomposition stage play an important role in oxidative spontaneous combustion [29–31], therefore, the stages Ⅱ and Ⅲ were considered to investigate the kinetic parameters in this paper. According to the above division principles, the characteristic temperatures corresponding to the respective stages of the six coal samples are summarized in Table 2.

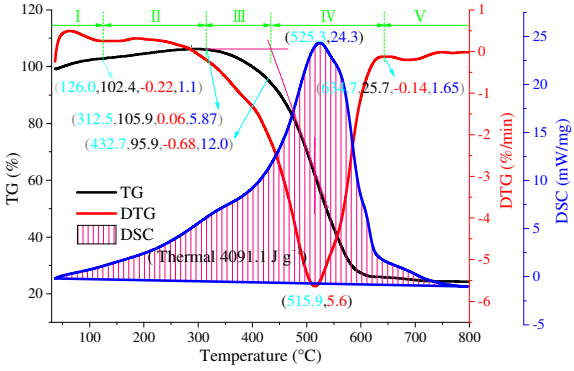

Fig. 1. The pyrolysis curve of the EBTC.

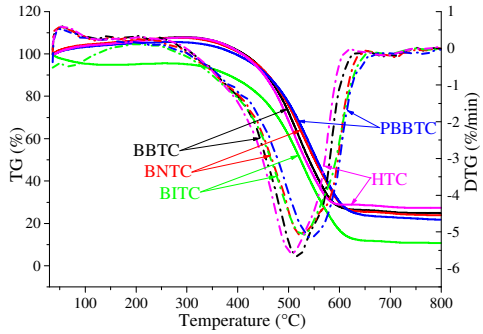

Fig. 2. TG and DTG curves of subsamples.

Table 2. Characteristic temperature points of coal samples

Sample	T_1, °C	T_2, °C	T_3, °C	T_4, °C	T_a, °C	T_b, °C	T_c, °C
EBTC	128.0	312.4	432.7	648.2	483.5	525.3	583.6
BBTC	126.5	287.1	443.8	653.0	487.8	526.9	586.3
BNTC	126.6	290.3	446.2	655.4	491.6	538.7	605.9
BITC	145.2	297.1	438.9	665.2	486.6	539.3	610.2
PBBTC	126.3	278.4	445.3	650.6	490.7	550.3	607.8
HTC	111.0	267.8	418.2	622.4	475.2	516.3	582.3

T_2 is the temperature at which the coal sample mass ratio is at a maximum point. In the oxygen absorption and mass gain stage of the low temperature oxidation process, the mass change of coal sample was mainly affected by the combined effect of coal oxygen composite mass gain and reaction consumption mass loss. With the increase of temperature, the oxidation process of coal samples accelerated, and the active groups in the coal molecular structure accumulated to a certain extent. The reaction consumption began to increase drastically. After T_2, the active groups began to participate in large-scale reactions. Then the rate of mass gain of the coal sample began to decrease. Table 2 shows that the T_2 temperature value of the treated coal sample increased; the coal sample was treated with [EMIm][BF_4] which reaches the maximum value: 44.6 °C higher than the HTC. The T_2 values of the BBTC and PBBTC did not change much, indicating the inhibition effectiveness had not diminished. The above situations might occur because the ILs destroyed the reactive functional groups, and it was more difficult to carry out the reaction when the coal molecule contained fewer functional groups. Therefore, more energy was required and the corresponding temperature point rose.

When the temperature of the coal sample exceeded T_3, the molecular structure of the coal began to decompose drastically, and a large amount of CO, CO_2, and small molecular organic gases were generated, releasing a large amount of thermal, and the mass of the coal began to drop drastically and started to burn. In the six coal samples, the HTC started to ignite at the lowest temperature, indicating that the ILs can inhibit the combustion ability of the coal sample. The ignition temperature was related to the number of reactive functional groups in the coal molecules, which meant that the active functional groups of the coal were subjected to the ILs damage. The T_3 of the sample was arranged in order of BNTC>PBBTC>BBTC>BITC>EBTC>HTC. Among them, the BNTC reached the highest ignition point, indicating that the BNTC was the most difficult to combust. The coal samples had different ignition temperatures, indicating that the damage to the active structure of coal molecules was also different.

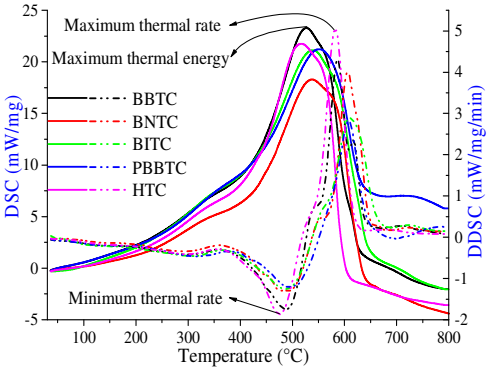

Fig. 3. DSC and DDSC curves for subsamples.

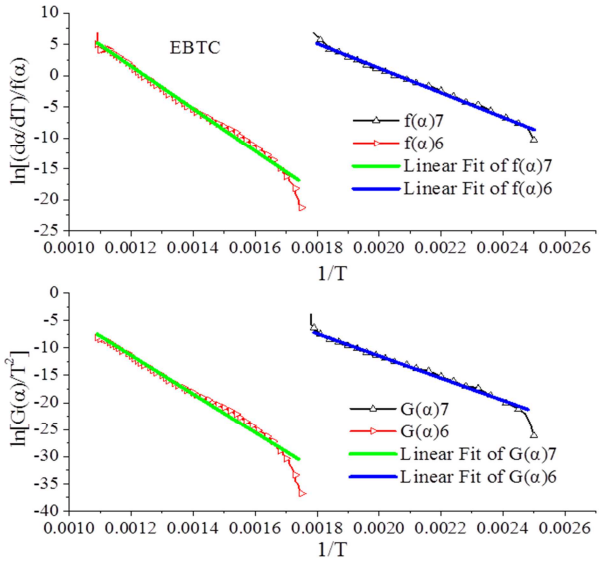

Fig.4. Fitting curves of EBTC at stages Ⅱ and Ⅲ.

At T_4 the coal sample was almost completely burned out with residual ash. The T_4 of HTC had the lowest temperature because the HTC had more active molecular structures on the surface of the molecule, so it can be burned out at a lower temperature. In addition, this further illustrated that the IL had caused damage to the coal molecular structure. In other coal samples treated with ILs, coal molecules contained fewer reactive functional groups. Therefore, it required higher temperature and more energies to completely burn out.

The heat flow curves of six coal samples were observed and analyzed during the oxidation, in which appeared the same exothermic trend. T_a was the minimum enthalpy rate, T_b represented the maximum enthalpy, T_c was maximum enthalpy rate. The T_a, T_b, and T_c of the six samples are summarized in Table 2. The values of the treated sample increased. BNTC, PBBTC, and BITC contained the highest T_a, T_b, and T_c, which were 16.4, 34.0, and 27.9 °C higher than HTC sample, respectively. This revealed that the inhibited samples required more energy to be completely burned because some of the reactive functional groups were destroyed by the ILs. The remaining molecules in the surface of the coal sample were reactive functional groups that were hardly to oxidize, so more energy was required to react.

Characterization of coal sample mass loss

From the oxygen absorption mass gain of the coal sample to the mass loss of combustion, the TG curve reflected the change of the mass of the coal sample at each temperature point. Therefore, compared with the HTC, the dissolution and destruction of the surface functional group of the coal by the IL could be analyzed. On the TG curve, each coal sample showed different trends of mass loss and mass gain at different temperature points caused by physical adsorption and chemical reaction of coal oxygen [32]. The solvency of the ILs to each activated functional group in the coal could be reflected in the TG curve according to the ratio of the mass loss. As the temperature increased, the active oxygen-absorbing active molecules in the coal first showed a strong reaction to oxygen molecules, which was manifested by an increase in oxygen uptake, at which the mass of the coal increased. The mass increase ratio and the mass loss ratio at each stage for coal samples are summarized in Table 3.

Table 3. The mass increase ratio and the mass loss ratio at each stage for coal samples

Sample	Stage Ⅰ	Stage Ⅱ		Stage Ⅲ and stage Ⅳ	
	TR^a, °C	TR^a, °C	Mass increase ratio, %	TR^a, °C	Mass loss ratio, %
EBTC	<128.0	128.0–312.4	0.82	312.4–648.2	7.06
BBTC	<126.5	126.5–287.1	0.30	287.1–653.1	8.01
BNTC	<126.6	126.6–290.3	0.07	290.3–655.4	7.72
BITC	<145.2	145.2–297.1	0.04	297.1–665.2	6.68
PBBTC	<126.3	126.3–278.4	0.04	278.4–680.6	5.68
HTC	<111.0	111.0–267.8	0.32	267.8–622.4	8.10

TR^a is temperature range

At the water evaporation stage, the treated coal sample required a higher temperature than the HTC, indicating that adsorption of water in the molecular structure of the coal samples treated with ILs required a higher temperature to evaporate completely. The mass gain ratio of HTC was relatively larger than other coal samples, indicating that there were more functional groups in coal molecules that are more likely to absorb oxygen. At the stage of thermal decomposition and loss of combustion, the mass loss ratio of HTC was the largest, indicating that the coal sample treated by ILs was more difficult to decompose during the thermal decomposition process.

Characteristics of oxidation kinetics of coal sample

The reaction of pulverized coal during thermo-gravimetric analysis was a heterogeneous solid-state reaction and it could be described by Eqs 1and 2 [33]:

Achar differential method:
$$\ln\frac{d\alpha/dT}{f(\alpha)} = \ln\frac{A}{\beta} - \frac{E_a}{RT} \tag{1}$$

Coast-Redfern integration method:
$$\ln\frac{G(\alpha)}{T^2} = \ln\left(\frac{AR}{\beta E_a}\right) - \frac{E_a}{RT} \tag{2}$$

where α is the degree of conversion, $f(\alpha)$ and $G(\alpha)$ are functions called the "reaction model" that describes the dependence of the reaction rate on the reaction's extent, A represents the pre-exponential Arrhenius factor, E_a is the apparent activation energy, T is the temperature , R is the gas constants and β is heating rate.

Many methods exist for kinetics analysis and 18 general solid reaction mechanism functions were selected in this paper [34,35]. At a constant heating rate, $\ln[(d\alpha/dT)/f(\alpha)]$ and $\ln[G(\alpha)/T^2]$ are linear with $1/T$. The E_a is determined from the slope of a plot of $\ln[(d\alpha/dT)/f(\alpha)]$ and $[G(\alpha)/T^2]$ against $1/T$. The corresponding pre-exponential factors (A) and correlation coefficients are derived from the intercept of the fitted curve. If the E_a and A (or ln$A$) values obtained by the integral and differential methods are supposed to be similar, a straight line with excellent linear relationship is necessarily obtained (represented by the correlation coefficient R). Then, the selected $G(\alpha)$ and $f(\alpha)$ are also the most suitable mechanism function for this reaction. The integral and differential curves of coal samples are achieved by plotting $\ln[(d\alpha/dT)/f(\alpha)]$ and $\ln[G(\alpha)/T^2]$ with 1/T, and fitting to obtain relevant parameters. Figure 4 shows the fitting curves of the coal samples at the stage of oxygen absorption mass increase stage and mass loss. Tables 4 and 5 summarize the kinetic parameters determined by integration and differentiation in the stages of oxygen absorption mass increase stage and mass loss.

Table 4. Kinetic parameters of integral and differential of coal samples at stage Ⅱ

Sample	Integral				Differential			
	function	r	E_{a2g}, J/mol	$\ln A_{2g}$, $\ln(min^{-1})$	function	r	E_{a2f}, J/mol	$\ln A_{2f}$, $\ln(min^{-1})$
EBTC	7	0.988	173.5	42.6	7	0.957	179.3	46.7
BBTC	7	0.961	175.8	43.3	7	0.955	171.8	44.9
BNTC	7	0.977	177.1	44.2	7	0.981	168.7	44.7
BITC	7	0.97	309.7	75.7	7	0.969	289.5	72.9
PBBTC	6	0.947	128.8	32.4	6	0.966	115.4	19.4
HTC	5	0.954	96.9	22.6	5	0.977	85.6	22.4

Table 5. Kinetic parameters of integral and differential of coal samples at stage Ⅲ

Sample	Integral				Differential			
	function	r	E_{a3g}, J/mol	$\ln A_{3g}$, $\ln(min^{-1})$	function	r	E_{a3f}, J/mol	$\ln A_{3f}$, $\ln(min^{-1})$
EBTC	6	0.973	301.2	44.9	6	0.986	289.5	45.6
BBTC	7	0.98	400.9	60.3	7	0.984	393.4	61.5
BNTC	6	0.984	269.3	39.6	6	0.985	268.1	41.9
BITC	6	0.987	254.4	37.4	6	0.989	251.9	39.5
PBBTC	6	0.998	256.9	38.2	6	0.977	264.3	40.8
HTC	13	0.955	86.9	10.1	13	0.988	74.22	10.6

The curve fitting results of the six coal types were screened and analyzed. It shows that the coal sample has different reaction mechanism functions in the stages of oxygen absorption mass increase and mass loss. The mechanism functions of the coal sample treated by the ILs were also different. It illustrates that the active structure of the coal molecule was swollen and destroyed in the process of ILs treatment. The active groups that caused the coal to participate in the reaction during combustion appear at different characteristic temperature points. It was consistent with the performance of coal samples at characteristic temperatures. The amount of some reactive groups was reduced or disappeared, so the combustion mechanism changed when the coal underwent a

composite reaction. The oxidation kinetic parameters of the coal samples are listed in Table 6, and ΔE_a is the difference in apparent activation energy (E_a) between the treated coal sample and the treated water treated with distilled water.

The structural activity of coal molecules was determined by the E_a. The larger the value is, the smaller the reactivity was. The rate of the chemical reaction was determined by the A. The larger the value is, the greater the rate of chemical reaction is. As coal and oxygen reacted completely, thermal energy was concentrated, and the degree of reaction was severer. The E_a was gradually increased. The magnitude of the increase of the six types of coal samples was also different, which further explained the difference in molecular structure and the reaction mechanism. Therefore, the combustion mass loss had a higher E_a than the oxygen absorption mass increased. Table 6 displays that the E_a values of the coal samples treated with ILs increased, indicating that the ILs had an inhibitory effect on the coal samples, and the inhibiting ability was different. In the stage of oxygen absorption mass increase, the E_a was in the order of BITC>BBTC>BNTC>EBTC>PBBTC>HTC, revealing that the inhibitory ability of the IL was [BMIm][I]>[BMIm][BF_4]>[BMIm][NO_3]> [EMIm][BF_4]. Among the six samples, the value of E_a for the [BMIm][I] sample was 299.6 J/mol, which may have been due to the active structure in the molecule being the least compared to the other three ILs, resulting in a decrease in activation energy. It is concluded that [BMIm][I] had the strongest inhibiting effect. The order of inhibition was ranked as follows: [BMIm][BF_4]>[EMIm][BF_4]>[BMIm][NO_3]>[BMIm][I] in the stage of combustion mass loss; [BMIm][BF_4] had the strongest inhibitory. The combustion properties exhibited in the two oxidation stages were different, indicating that the IL's inhibition to coal was different at each stage.

Table 6. Oxidation kinetic parameters of coal samples

Sample	Stage Ⅱ				Stage Ⅲ			
	E_{a2}, J/mol	ΔE_{a2}, J/mol	$\ln A_2$, $\ln(min^{-1})$	r	E_{a3}, J/mol	ΔE_{a3}, J/mol	$\ln A_3$, $\ln(min^{-1})$	r
EBTC	161.4	70.2	44.6	0.968	295.4	214.9	45.3	0.979
BBTC	173.8	85.5	44.1	0.958	397.2	316.7	60.9	0.98
BNTC	172.9	81.6	44.4	0.979	268.7	188.3	40.7	0.984
BITC	299.6	208.3	74.3	0.969	253.2	172.7	38.5	0.988
PBBTC	122.1	30.9	25.9	0.956	260.6	180.1	39.5	0.983
HTC	91.3	0	22.5	0.965	80.5	0	10.4	0.971

CONCLUSIONS

The T_1, T_2, T_3, T_4, T_a, T_b, and T_c of the coal samples treated with the IL increased, and the characteristic temperature of the coal sample treated by the [BMIm][I] increased the mos,t which increased 34.2, 29.3, 20.7, 42.8, 11.4, 23.0, and 27.9 °C, respectively. Coal samples treated with ILs required higher temperatures for water evaporation and oxygen gain, and the mass gain ratios increased and decreased during the evaporation and thermal decomposition stages, indicating that the IL treated coal samples were much harder to decompose.

The E_a of the coal sample treated by ILs increased, and the mechanism function also changed accordingly, indicating that the ILs could improve the thermal stability of the coal sample in the oxygen absorption and mass gain stage and the combustion mass loss stage. In the oxygen absorption and mass increase stage, the inhibitory properties of the four ILs were as follows: [BMIm][I]>[BMIm][BF_4]>[BMIm][NO_3]>[EMIm][BF_4]. In the stage of combustion mass loss, the

inhibition effectiveness was ranked as: [BMIm][BF_4]>[EMIm][BF_4]>[BMIm][NO_3]>[BMIm][I]. Moreover, the ILs inhibited the combustion reaction of coal was carried out in stages, and exhibited different properties at various stages.

Samples treated with the same IL one month earlier and one month later exhibited essentially the same properties during combustion. Compared with the comparative sample, it also showed an increase in characteristic temperature, an increase in E_a, and a change in the mechanism function. This indicated that the inhibition effectiveness of the IL on the coal sample hardly decreased with time.

ACKNOWLEDGMENTS

This work was sponsored by the International Science and Technology Cooperation and Exchange of Shaanxi Province (Grant no. 2016KW-070), the Shaanxi Province Innovative Talent Promotion Plan-Youth Science and Technology New Star Project (No. S2019-ZC-XXXM-0037), and and National Key Research and Development Plan of China (No. 2018-YFC-0807900).

REFERENCES

[1] C. Kuenzer, G.B. Stracher, Geomorphology of coal seam fires, Geomorphology 138 (2012) 209–222.

[2] Z.Y. Song, C. Kuenzer, Coal fires in China over the last decade: A comprehensive review, Int. J. Coal Geol. 133 (2014) 72–99.

[3] D.M. Wang, G.L. Dou, X.X. Zhong, H.H. Xin, B.T. Qin, An experimental approach to selecting chemical inhibitors to retard the spontaneous combustion of coal, Fuel 117 (2014) 218–223.

[4] J.H. Li, Z.H. Li, Y.L. Yang, B. Kong, C.J. Wang, Laboratory study on the inhibitory effect of free radical scavenger on coal spontaneous combustion, Fuel Process. Technol. 171 (2018) 350–360.

[5] J.H. Li, Z.H. Li, C.J. Wang, X.Y. Zhang, Experimental study on the inhibitory effect of ethylenediaminetetraacetic acid (EDTA) on coal spontaneous combustion, Fuel Process. Technol. 2018, 178.

[6] C.Y. Hao, Y.L. Chen, J.R. Wang, C.B. Deng, G. Xu, F.W. Dai, R. Si, H.F. Wang, H.Y. Wang, Study on the effect of iron-based deoxidizing inhibitors for coal spontaneous combustion prevention, Energies 11 (2018) 789.

[7] J.H. Li, Z.H. Li, Y.L. Yang, X.Y. Zhang, D.C. Yan, L.W. Liu, Inhibitive effects of antioxidants on coal spontaneous combustion, Energy Fuels 31 (2017) 14180–14190.

[8] W.M. Cheng, X.M. Hu, J. Xie, Y.Y. Zhao, An intelligent gel designed to control the spontaneous combustion of coal: Fire prevention and extinguishing properties, Fuel 210 (2017) 826–835.

[9] Y. Yang, Y.T. Tsai, Y.N. Zhang, C.M. Shu, J. Deng, Inhibition of spontaneous combustion for different metamorphic degrees of coal by Zn/Mg/Al-CO3-layered double hydroxide, Process Saf. Env. Prot. 113 (2017) 401–412.

[10] J. Deng, Y. Yang, Y.N. Zhang, B. Liu, C.M. Shu, Inhibiting effects of three commercial inhibitors in spontaneous coal combustion, Energy 160 (2018) 1174–1185.

[11] D.M. Wang, H.H. Xin, X.Y. Qi, G.L. Dou, G.S. Qi, L.Y. Ma, Reaction pathway of coal oxidation at low temperatures: a model of cyclic chain reactions and kinetic characteristics, Combust. Flame 163 (2016) 447–460.

[12] B. Li, G. Chen, H. Zhang, C.D. Sheng, Development of non-isothermal TGA–DSC for kinetics analysis of low temperature coal oxidation prior to ignition, Fuel 118 (2014) 385–391.

[13] P.V. Kortunov, L.S. Baugh, M. Siskin, Pathways of the chemical reaction of carbon dioxide with Ionic Liquids and amines in ionic liquid solution, Energy Fuels 29 (2015) 5990–6007.

[14] W.Q. Zhang, S.G. Jiang, Z.Y. Wu, K. Wang, H. Shao, T. Qin, X. Xi, H.b. Tian, Influence of imidazolium-based ionic liquids on coal oxidation, Fuel 217 (2018) 529–535.

[15] J. Cummings, S. Kundu, P. Tremain, B. Moghtaderi, R. Atkin, K. Shah, Investigations into physicochemical changes in thermal coals during low-temperature ionic liquid Treatment, Energy Fuels 29 (2015) 7080–7088.

[16] J. Cummings, P. Tremain, K. Shah, E. Heldt, B. Moghtaderi, R. Atkin, S. Kundu, H. Vuthaluru, Modification of lignites via low temperature ionic liquid treatment, Fuel Process. Technol. 155 (2017) 51–58.

[17] Z.P. Lei, Y.Q. Zhang, L. Wu, H.F. Shui, Z.C. Wang, S.B. Ren, The dissolution of lignite in ionic liquids, RSC Adv. 3 (2013) 2385–2389.

[18] Z.P. Lei, L.L. Cheng, S.F. Zhang, Y.Q. Zhang, H.F. Shui, S.B. Ren, Z.C. Wang, Dissolution performance of coals in ionic liquid 1-butyl-3-methyl-imidazolium chloride, Fuel Process. Technol. 129 (2015) 222–226.

[19] K. Shah, R. Atkin, R. Stanger, T. Wal, B. Moghtaderi, Interactions between vitrinite and inertinite-rich coals and the ionic liquid – [bmim][Cl], Fuel 119 (2014) 214–218.

[20] P. Painter, N. Pulati, R. Cetiner, M. Sobkowiak, G. Mitchell, J. Mathews, Dissolution and dispersion of coal in ionic liquids, Energy Fuels 24 (2010) 1848–1853.

[21] P. Painter, R. Cetiner, N. Pulati, M. Sobkowiak, J. Mathews, Dispersion of liquefaction catalysts in coal using ionic liquids, Energy Fuels 24 (2010) 3086–3092.

[22] Y. Li, X.P. Zhang, S.Y. Lai, H.F. Dong, X.L. Chen, X.L. Wang, Y. Nie, Y. Sheng, S.J. Zhang, Ionic liquids to extract valuable components from direct coal liquefaction residues, Fuel 94 (2012) 617–619.

[23] Z.P. Lei, L.L. Wu, Y.Q. Zhang, H.F. Shui, Z.C. Wang, C.X. Pan, H.P. Li, S.B. Ren, S.G. Kang. Microwave-assisted extraction of Xianfeng lignite in 1-butyl-3-methyl-imidazolium chloride, Fuel 95 (2012) 630–633.

[24] L.Y. Wang, Y.L. Xu, S.G. Jiang, M.G. Yu, T.X. Chu, W.Q. Zhang, Z.Y. Wu, L.W. Kou, Imidazolium based ionic liquids affecting functional groups and oxidation properties of bituminous coal, Saf. Sci. 50 (2012) 1528–1534.

[25] W.Q. Zhang, S.G. Jiang, C. Hardacre, P.Goodrich, K.Wang, Z.Y. Wu, H. Shao, Inhibitory effect of phosphonium-based ionic liquids on coal oxidation, Energy Fuels 28 (2014) 4333–4441.

[26] W.Q. Zhang, S.G. Jiang, Z.Y. Wu, K. Wang, H. Shao, T. Qin, X. Xi, H.B. Tian, Influence of imidazolium-based ionic liquids on coal oxidation, Fuel 217 (2018) 529–535.

[27] F.S. Cui, B. Laiwang, C.M. Shu, J.C. Jiang, Inhibiting effect of imidazolium-based ionic liquids on the spontaneous combustion characteristics of lignite, Fuel 217 (2018) 508–514.

[28] R.L. Vekariya, A review of ionic liquids: Applications towards catalytic organic transformations, J. Mol. Liq. 227 (2017) 44–60.

[29] J. Deng, Z.J. Bai, Y. Xiao, Effects on the activities of coal microstructure and oxidation treated by imidazolium-based ionic liquids, J. Therm. Anal. Calorim. 133 (2018) 453–463.

[30] J. Deng, B. Li, Y. Xiao, L. Ma, C.P. Wang, B. Laiwang, C.M. Shu, Combustion properties of coal gangue using thermogravimetry–Fouriertransform infrared spectroscopy, Appl. Therm. Eng. 116 (2017) 244–252.

[31] J. Deng, Q.W. Li, Y. Xiao, H. Wen, The effect of oxygen concentration on the non-isothermal combustion of coal, Thermochim. Acta 653 (2017) 106–115.

[32] B. Li, G. Chen, H. Zhang, C.D. Sheng, Development of non-isothermal TGA–DSC for kinetics analysis of low temperature coal oxidation prior to ignition, Fuel 118 (2014) 385–391.

[33] X.Y. Qi, Q.Z. Li, H.H. Zhang, H.H. Xin, Thermodynamic characteristics of coal reaction under low oxygen concentration conditions, J. Energy Inst. 90 (2017) 544–555.

[34] S. Vyazovkin, A. K. Burnham, J. M. Criado, L. A. Pérez-Maqueda, C. Popescu, N. Sbirrazzuoli, ICTAC Kinetics Committee recommendations for performing kineticcomputations on thermal analysis data, Thermochim. Acta 520 (2011) 1–19.

[35] G. Chen, X.Q. Ma, M.S. Lin, Y.Z. Lin, Z.S. Yu, Study on thermochemical kinetic characteristics and interaction during low temperature oxidation of blended coals, J. Energy Inst. 88 (2015) 221–228.